Title	Rotational symmetry breaking in the ground state of sodium-doped cuprate superconductors
Author(s)	Chen, Y; Rice, TM; Zhang, FC
Citation	Physical Review Letters, 2006, v. 97 n. 23
Issued Date	2006
URL	http://hdl.handle.net/10722/45245
Rights	Physical Review Letters. Copyright © American Physical Society.

Rotational Symmetry Breaking in the Ground State of Sodium-Doped Cuprate Superconductors

Yan Chen
Department of Physics and Center of Theoretical and Computational Physics, The University of Hong Kong, Pokfulam Road, Hong Kong, China

T. M. Rice
Department of Physics and Center of Theoretical and Computational Physics, The University of Hong Kong, Pokfulam Road, Hong Kong, China and Institut für Theoretische Physik, ETH-Zürich, CH-8093 Switzerland

F. C. Zhang
Department of Physics and Center of Theoretical and Computational Physics, The University of Hong Kong, Pokfulam Road, Hong Kong, China and Department of Physics, Zhejiang University, Hangzhou, China

(Received 18 July 2006; published 6 December 2006)

We use an extended t-J model to study a single hole bound to a Na^+ acceptor in $Ca_{2-x}Na_xCuO_2Cl_2$. For parameters suitable to cuprates, the ground state has a twofold degeneracy, corresponding to even (odd) reflection symmetry around the x (y) axes. The conductance pattern of the broken symmetry state is anisotropic as the tip of a tunneling microscope scans above the Cu-O-Cu bonds along the x (y) axes. This anisotropy is pronounced at lower voltages but reduced at higher voltages. Our theory agrees qualitatively with recent data of scanning tunneling microscopy showing broken local rotational symmetry.

DOI: 10.1103/PhysRevLett.97.237004 PACS numbers: 74.72.−h, 74.25.Jb, 74.62.Dh

The recent atomically resolved scanning tunneling microscopy (STM) studies by Davis and collaborators [1,2] on strongly underdoped $Ca_{2-x}Na_xCuO_2Cl_2$ revealed a surprisingly complex pattern with the square symmetry of the lattice broken on a local scale. The STM data were analyzed to obtain the local hole density of Cu-site using the method proposed by Randeria, Sensarma, Trivedi, and Zhang [3] and also a related method proposed by Anderson and Ong [4]. In these methods, the differential conductance signal is integrated from the chemical potential to a substantial voltage cutoff. Randeria *et al.* [3] pointed out that the ratio between its positive voltage (electron injection) and negative voltage (hole injection) signals measured the local hole density of the Cu-site independent of the strength of the troublesome tunneling matrix elements.

In $Ca_{2-x}Na_xCuO_2Cl_2$, the acceptor Na^+-ions substitute for Ca^{2+}-ions and sit in the center of a square of four Cu sites both above and below the outermost CuO_2 layer. The attractive potential for the doped holes generated by a Na^+-acceptor does not break the local square symmetry. The broken local square lattice symmetry observed in the STM data is most pronounced at the in-plane oxygen sites and for a lower voltage cutoff. This raises an interesting question about the origin of this broken local square symmetry.

In this Letter, we address this question and show that such broken symmetry states appear in the case of a hole confined to a cluster of sites centered at a Na^+-acceptor. Further, this broken local symmetry shows up in the STM mapping primarily as a modulation pattern above the O-sites in the outermost CuO_2-layer.

We start by considering the STM tunneling process in detail in $Ca_{2-x}Na_xCuO_2Cl_2$. As pointed out by Rice and Tsunetsugu [5], the STM tip couples primarily to the $3p_z$-states of the outermost Cl layer, but the matrix element to tunnel directly into a hole located on the CuO_2 square directly underneath the Cl-ion vanishes by symmetry. The holes move in a band of singlets with $d_{x^2-y^2}$-symmetry centered on Cu sites but strongly hybridized with the four nearest-neighboring (NN) O sites. The $3p_z$-Cl states, however, hybridize with the hole states centered on the four NN Cu sites [6] through the direct overlap of the $3p_z$-Cl with $2p_{x(y)}$-O orbitals and also through the $4s$-Cu orbital on the site directly below each Cl. The amplitude to inject an electron in a $3p_z$-Cl hole wave function is a superposition of hole states centered on the four NN Cu-sites (see Fig. 1).

$$p^\dagger_{\mathrm{Cl},\mathbf{i},\sigma}|\Psi_0^{1h}\rangle \propto \sum_\tau \langle \mathbf{i}, \mathrm{Cl}|\mathbf{i}+\tau, \mathrm{Cu}\rangle c^\dagger_{\mathbf{i}+\tau,\sigma}|\Psi_0^{1h}\rangle \propto \sum_\tau (-1)^{M_\tau} c^\dagger_{\mathbf{i}+\tau,\sigma}|\Psi_0^{1h}\rangle \quad (1)$$

where $p^\dagger_{\mathrm{Cl},\mathbf{i},\sigma}(c^\dagger_{\mathbf{i}+\tau,\sigma})$ are creation operators for electrons in the $3p_z$-Cl orbital at site $\mathbf{i}$ (planar coordinate) and the d-p hybridized orbital centered on the Cu-site at $\mathbf{i}+\tau$ in the outermost CuO_2 layer, respectively, with $\langle \mathbf{i}, Cl|\mathbf{i}+\tau, Cu\rangle$ as their overlap, $\tau = \pm\mathbf{x}, \pm\mathbf{y}$ is a planar vector connecting NN Cu sites, and $|\Psi_0^{1h}\rangle$ denotes the single-hole ground state with energy E_0^{1h}. Assuming the square lattice is four-fold rotational invariant, the overlaps are independent of $\vec{\tau}$ except for their sign, leading to Eq. (1). For $d_{x^2-y^2}$ symmetry of the Cu-orbital, we have $(-1)^M = -1$

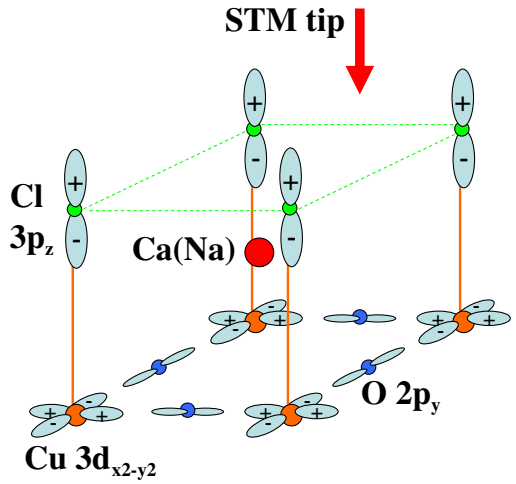

FIG. 1 (color online). Schematic crystal structure of $Ca_{2-x}Na_xCuO_2Cl_2$ around a Ca^{2+} ion or a doped Na^+ ion. The sign represents the phase of the Cu- and Cl-orbital wave function.

for $\tau = \pm\mathbf{x}$, and $(-1)^M = +1$ for $\tau = \pm\mathbf{y}$. Note that only the relative phase is important.

Following the theory of STM tunneling developed by Tersoff and Hamann [7], we write the differential conductance at voltage V at $\mathbf{r}$, the center of curvature of the tip as

$$\frac{dI(\mathbf{r})}{dV} \propto \sum_{\sigma,m} |\langle m|a^\dagger_{\mathbf{r},\sigma}|\Psi_0^{1h}\rangle|^2 \delta(\omega - E_m + E_0^{1h}) \quad (2)$$

where $a^\dagger_{\mathbf{r},\sigma}$ is the electron creation operator at position $\mathbf{r}$, $|m\rangle$ are eigenstates of the half-filled system with energy E_m, and $\omega =$ eV. When the tip is scanned from above the Cl site at $\mathbf{i}$ to a NN site, $\mathbf{i} + \tau'$, we have

$$a^\dagger_{\mathbf{r},\sigma}|\Psi_0^{1h}\rangle = [\langle \mathbf{r}|\mathbf{i}, \mathrm{Cl}\rangle p^\dagger_{\mathrm{Cl},\mathbf{i},\sigma} + \langle \mathbf{r}|\mathbf{i} + \tau', \mathrm{Cl}\rangle p^\dagger_{\mathrm{Cl},\mathbf{i}+\tau',\sigma}]|\Psi_0^{1h}\rangle. \quad (3)$$

The integrated current at $\mathbf{r}$ up to a positive voltage V is then,

$$I(\mathbf{r}, \omega) \propto \sum_{\sigma,m} \Big| \langle m| \sum_\tau (-1)^{M_\tau} [\langle \mathbf{r}|\mathbf{i}, \mathrm{Cl}\rangle c^\dagger_{\mathbf{i}+\tau,\sigma} + \langle \mathbf{r}|\mathbf{i} + \tau', \mathrm{Cl}\rangle c^\dagger_{\mathbf{i}+\tau'+\tau,\sigma}]|\Psi_0^{1h}\rangle \Big|^2 \times \Theta(\omega - E_m + E_0^{1h}) \quad (4)$$

where Θ is a step function. The variation of the tunneling current as one scans between two NN Cl sites is sensitive to the relative phase to inject electrons on NN Cu sites in $|\Psi_0^{1h}\rangle$. The important role of quantum interference effect in interpreting STM images has also been discussed for multiple tunneling channels on sulfur surfaces [8]. To this end, we examine the lowest energy single hole states for clusters up to 16 Cu-sites including an attractive acceptor potential in the center square.

The two-dimensional t-t'-J model for the cluster is defined by the Hamiltonian,

$$\mathcal{H} = -\sum_{i,\sigma} \epsilon_i c^\dagger_{i\sigma} c_{i\sigma} - t \sum_{\langle i,j\rangle\sigma} (c^\dagger_{i\sigma} c_{j\sigma} + \mathrm{H.c.}) - t' \sum_{\langle\langle i,j\rangle\rangle\sigma} (c^\dagger_{i\sigma} c_{j\sigma} + \mathrm{H.c.}) + J \sum_{\langle i,j\rangle} \mathbf{S}_i \cdot \mathbf{S}_j. \quad (5)$$

A constraint of no double electron occupation is implied. $\langle i, j\rangle$ and $\langle\langle i, j\rangle\rangle$ refer to NN and next-nearest-neighbor (NNN) sites i and j. The on site potential of the four NN Cu sites of the Na^+-acceptor is $\epsilon_i = \epsilon_s$, while $\epsilon_i = 0$ for the rest of the sites. The single-hole ground state of Eq. (5) with $t' = 0$ was obtained previously using exact diagonalization for small clusters by von Szczepanski *et al.* [9], Rabe and Bhatt [10], and Gooding [11]. The ground state with spin $S = 1/2$ was found to be orbitally doubly degenerate in certain parameter regimes [10–12]. When a NNN hopping t' is included, our results below show that the doubly degenerate $S = 1/2$ states are lowest in energy within a reasonable parameter range. The symmetry of the lowest energy state however is sensitive to boundary condition and parameters. In our calculations, we choose $t = 1$ and $J = 0.3$, suitable for the cuprates, and study the ground state as a function of t' and ϵ_s in clusters of 12- and 16-sites (see Fig. 2).

Exact diagonalization of small t-t'-J clusters has been reported earlier [13–16]. For a $16 - (4 \times 4)$ site cluster with periodic boundary condition (PBC), the ground state of a single hole has a four-fold symmetry with hole momentum $(\pm\pi/2, \pm\pi/2)$ if $t' < 0$, and a twofold symmetry with hole momentum $(\pi, 0)$ or $(0, \pi)$ if $t' > 0$. The impurity potential affects not only the local charge and spin distributions but also the symmetry of the ground state wave function [10,11]. In this study, we focus on the reflection symmetries with respect to x and y axes passing through the sodium dopant (P_x and P_y, respectively). Since $[P_{x(y)}, H] = 0$, we may classify states according to the quantum numbers of P_x, P_y. We denote the state with $(P_x, P_y) = (+1, -1)$ as phase (I), and the doubly degenerate states $(+1, -1)$ and $(-1, +1)$ as phase (II), and $(-1, -1)$ as phase (III). In Figs. 3(a) and 3(b), we show the

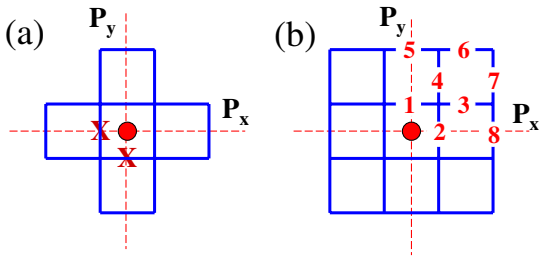

FIG. 2 (color online). The configuration of 12-site (a) and 16-site cluster (b). The dashed line corresponds to the reflection axis for $P_{x(y)}$. The cross marks the tip position on the middle point of two NN Cu sites along the x and y axes. In (b), eight independent bonds are labeled with numbers.

ground state phase diagram a regime with the doubly degeneracy obtained by exact diagonalization. A band structure calculation [17] and angle resolved photoemission experiments [18] both indicate a rather weak $t' \approx -0.1$ for $Ca_{2-x}Na_xCuO_2Cl_2$. Thus we expect the existence of doubly degenerate ground state in this material. We note that the four low-lying states with different reflection symmetries are very close in energy. Small perturbation of lattice geometry, boundary condition, t', or ϵ_s may change symmetry of the groundstate, e.g., in Fig. 3(c), we show the energy level evolution as ϵ_s changes for a fixed value of $t' = -0.12$.

Next we examine the effect of the broken rotational symmetry ground state on the STM measurements. We consider the system to be in one of the two degenerate states, say $(+1, -1)$ due to quadruple interaction of two single-hole states or other couplings. Note the local density of states at the Cu sites remains rotationally symmetric in this state. However, because of the interference between different Cu sites to the integrated differential conductance in Eq. (4), the STM tip at a position between NN Cu sites breaks rotational symmetry. Consider the tip positions above the two geometrically symmetric points halfway between the Cu site $\mathbf{i}$ and its NN sites $\mathbf{i}+\mathbf{x}$ or $\mathbf{i}+\mathbf{y}$ with a Na^+-acceptor located at $\mathbf{i}+\mathbf{x}/2+\mathbf{y}/2$. Since $\langle \mathbf{r}|\mathbf{i}, \mathrm{Cl}\rangle = \langle \mathbf{r}|\mathbf{i}+\tau', \mathrm{Cl}\rangle$ for the midpoint $\mathbf{r}$, the integrated differential conductance $I^{x(y)}(\omega) = I(\frac{\mathbf{x}}{2}(\frac{\mathbf{y}}{2}), \omega)$ at position $\mathbf{i}+\frac{\mathbf{x}}{2}(\frac{\mathbf{y}}{2})$ with the cutoff energy ω is

$$I^{x(y)}(\omega) = \sum_\sigma I_\sigma^{x(y)}(\omega),$$
$$I_\sigma^{x(y)}(\omega) \propto \sum_m |\langle m| \sum_\tau (-1)^{M_\tau} (c^\dagger_{\mathbf{i}+\tau,\sigma} + c^\dagger_{\mathbf{i}+\mathbf{x(y)}+\tau,\sigma})|\Psi_0^{1h}\rangle|^2 \Theta(\omega - E_m + E_0^{1h}), \quad (6)$$

where I_σ is the spin-dependent integrated differential conductance. This conductance can be calculated by diagonalizing the Hamiltonian in Eq. (5) to obtain $|\Psi_0^{1h}\rangle$ and also all the eigenstates $|m\rangle$ with energies E_m at half-filling. Note that $I^x(\omega) = I^y(\omega)$ by symmetry if $|\Psi_0^{1h}\rangle$ is nondegenerate. In the parameter regime where $|\Psi_0^{1h}\rangle$ is doubly degenerate (see Fig. 2), I^x and I^y can be different. In Fig. 4(a), we plot $I^x(\omega)$ and $I^y(\omega)$ versus the cutoff energy ω obtained from the 12-site cluster calculations, for a hole ground state with symmetry $(+1, -1)$ and spin $S_z = 1/2$. The asymmetry of I between the two tip scans is apparent and is more pronounced at a lower ω and becoming weaker at higher ω. To see the asymmetry more clearly, we also plot the ratio of the conductances at the two tip points,

$$\eta(\omega) = I^x(\omega)/I^y(\omega). \quad (7)$$

It is interesting to note the strong cutoff energy dependence of the asymmetry in the conductance. For example, $\eta \approx 0.3$ for $\omega \approx J$, rises to $\eta \approx 0.85$ at $\omega = 4J$. As $\omega \to \infty$, $\eta \approx 1.04$, showing only very weak asymmetry. Our results are consistent with the recent STM observation [1], where strong asymmetry has been found at a lower $\omega = 150$ meV ($\sim J$), much weaker or unobservable asymmetry at $\omega = 600$ meV ($\sim 4J$). In Fig. 4(b) and 4(c), we show the spin-dependent conductances $I_\sigma(\tau'/2, \omega)$ as functions of ω in different spin channels. Our theory predicts that the asymmetry is spin-dependent. In the high ω limit, the ratio $I^x_\uparrow/I^y_\uparrow \sim 1.23$ in the spin-up channel and $I^x_\downarrow/I^y_\downarrow \sim 0.88$ in the spin-down channel. Compensation between two different spin singlet and triplet channels leads to weaker asymmetry in the total ratio, $I^x/I^y \sim 1.04$. However, rapid spin flip processes around the Na^+-acceptor may make spin-resolved STM experiments difficult. However, in very underdoped samples, the spin may be frozen around the

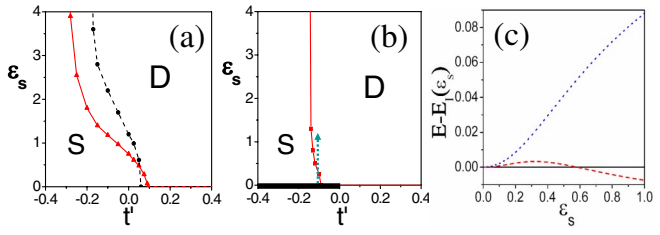

FIG. 3 (color online). Ground state phase diagram in the parameter space of t' and ϵ_s in (a) 12-site cluster (black dashed line) and 16-site cluster (solid line) with open boundary condition, (b) 16-site cluster with PBC. Regime D: the doubly degenerate state; regime S: the singly degenerate state. The thick black line in (b) corresponds to the four-fold symmetric states at $\epsilon_s = 0$. (c) Energy levels as functions of ϵ_s at $t' = -0.12$ as indicated by the dashed line in (b). E_I denotes the energy in phase I. The dashed line is for doubly degenerate states while the dotted line is for phase III.

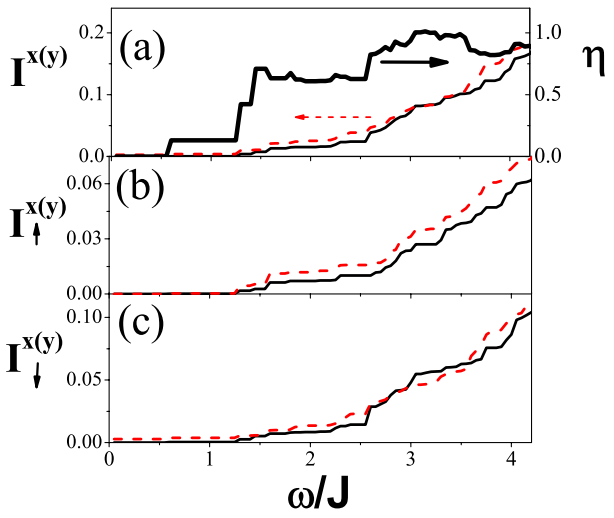

FIG. 4 (color online). The total integrated differential conductance on two cross (X) sites in Fig. 2(a) along the x- (solid line) and along the y-axis (dashed line) as functions of the cutoff energy ω together with the anisotropy ratio η (thick solid line). The results for spin-up channel (b), and spin-down channel (c). In the calculations (b) and (c), the single-hole state has a spin $S_z = 1/2$.

TABLE I. The hopping integral and spin-spin correlation function for various bonds in a 16-site cluster with PBC for $t' = -0.1$ and $\epsilon_s = 1.0$. The bonds are labeled in Fig. 2(b).

bond index	1	2	3	4	5	6	7	8
$\langle c_i^\dagger c_j \rangle$	0.342	0.328	0.122	0.129	0.020	0.014	0.012	0.016
$-\langle S_i S_j \rangle$	0.167	0.074	0.161	0.167	0.329	0.336	0.347	0.334

Na^+-acceptor so that spin-resolved STM experiments may be possible.

To better understand our results, we analyze the ground state and the conductance in a 4-site cluster. Altman and Auerbach [19] found that the single-hole ground state of a 4-site Hubbard model with moderate on-site repulsion U is twofold degenerate with spin-1/2. We study the single-hole ground state of the t-t'-J model and focus on the spin-1/2 sector. Note that the acceptor potential plays no role in the 4-site cluster. The ground state is doubly degenerate with the energy $E_g = -\frac{J}{2} - \sqrt{3t^2 + (t' + \frac{J}{2})^2}$, with reflection symmetries $(+1, -1)$ and $(-1, +1)$. Assuming the former to be ground state leads to (apart from an overall prefactor) $I_\uparrow^x(\omega) = \frac{4}{3}\cos^2\gamma\Theta(\omega - J)$, $I_\downarrow^x(\omega) = \frac{2}{3}\cos^2\gamma\Theta(\omega - J)$, $I_\uparrow^y(\omega) = 0$, and $I_\downarrow^y(\omega) = \cos^2\gamma\Theta(\omega) + \sin^2\gamma\Theta(\omega - 2J)$, with $\tan\gamma = \sqrt{3}t/(J + t' + E_g)$. Because of the nature of the many body wave function, the conductance in Eq. (6) may involve either destructive or constructive interference among different components, even an exact cancellation in the case of $I_\uparrow^y$. Summing over spins, gives $I^x(\omega) = I_\uparrow^x + I_\downarrow^x = 2\cos^2\gamma\Theta(\omega - J)$, while $I^y(\omega) = \cos^2\gamma\Theta(\omega) + \sin^2\gamma\Theta(\omega - 2J)$. It is obvious that $\eta(\omega)$ becomes infinite for $\omega \in (0, J)$, while $\eta(\omega) = 1/2$ for $\omega \in (J, 2J)$ and $\eta(\omega) = 2\cos^2\gamma$ for $\omega > 2J$. For $t'/t = -0.1$ and $\omega > 2J$, $\eta \sim 0.97$. Therefore, the asymmetry becomes rather weak with increasing bias voltage. The ratio of the integrated conductances in the $(-1, +1)$ ground state can be obtained by interchanging x and y and is given by η^{-1}. We have also calculated the integrated conductance for the hole injection tunneling and found it also to be rotational asymmetric as is the ratio between the electron injected and hole injected conductances.

In the broken rotational symmetry state, the local charge density at each of four NN Cu sites around a Na^+-acceptor is uniform, but the NN Cu-Cu bonding amplitudes are not equal. For instance, in the $(+1, -1)$ ground state of the 16-site cluster, the expectation values of hopping amplitude $\langle c_i^\dagger c_j \rangle$ as well as spin-spin correlation function $\langle S_i S_j \rangle$ for various bonds are listed in Table I. The hopping amplitude along bond 1 is slightly stronger than that of bond 2, while the spin-spin correlation function exhibits a much stronger asymmetry. If the acceptor leads to localization of holes a larger hopping amplitude and weaker spin-spin correlation function appear in its vicinity, but further away, the hole density becomes very small and the spin-spin correlation function approaches to -0.34. Localization can be strengthened by the electron-phonon interaction, and also the spin-coupling may favor polaron formation [20]. It will be interesting to examine possible polaron effects in the presence of the local broken symmetry.

The authors thank Y. Kohsaka and S. Davis for discussions of their experiments. Y. C. especially thanks P. W. Leung, T. K. Lee, H. Tsunetsugu, and M. Troyer for numerical assistance. Y. C. and F. C. Z. are supported by RGC grants (Nos. HKU-3/05C, HKU7054/05P, HKU7013/04P, and HKU7012/06P) from the HKSAR government, and T. M. R. by the MANEP program of the Swiss Nationalfonds.

[1] J. C. Davis, *KITP Miniprogram: Complexity in Strongly Correlated Electron Systems* (2005), website http://online.itp.ucsb.edu/online/complex05; (private communications).
[2] T. Hanaguri *et al.*, Nature (London) **430**, 1001 (2004).
[3] M. Randeria, R. Sensarma, N. Trivedi, and F. C. Zhang, Phys. Rev. Lett. **95**, 137001 (2005).
[4] P. W. Anderson and N. P. Ong, J. Phys. Chem. Solids **67**, 1 (2006).
[5] T. M. Rice and H. Tsunetsugu, Eur. Phys. J. B **49**, 1 (2006).
[6] I. Martin, A. V. Balatsky, and J. Zaanen, Phys. Rev. Lett. **88**, 097003 (2002).
[7] J. Tersoff and D. R. Hamann, Phys. Rev. B **31**, 805 (1985).
[8] M. A. Van Hove *et al.*, Prog. Surf. Sci. **54**, 315 (1997).
[9] K. J. von Szczepanski, T. M. Rice, and F. C. Zhang, Europhys. Lett. **8**, 797 (1989).
[10] K. M. Rabe and R. N. Bhatt, J. Appl. Phys. **69**, 4508 (1991).
[11] R. J. Gooding, Phys. Rev. Lett. **66**, 2266 (1991).
[12] The double degenerate ground state was not found in Ref. [9], due to the specific cluster they considered.
[13] E. Gagliano, S. Bacci, and E. Dagotto, Phys. Rev. B **42**, 6222 (1990).
[14] R. J. Gooding, K. J. E. Vos, and P. W. Leung, Phys. Rev. B **50**, 12 866 (1994).
[15] M. Troyer, H. Tsunetsugu, and T. M. Rice, Phys. Rev. B **53**, 251 (1996).
[16] C. T. Shih, Y. C. Chen, and T. K. Lee, Phys. Rev. B **57**, 627 (1998).
[17] L. F. Mattheiss, Phys. Rev. B **42**, 354 (1990).
[18] J. C. Ronning *et al.*, Science **282**, 2067 (1998).
[19] E. Altman and A. Auerbach, Phys. Rev. B **65**, 104508 (2002).
[20] P. Prelovsek, R. Zeyher, and P. Horsch, Phys. Rev. Lett. **96**, 086402 (2006).